HEAT TRANSFER PERFORMANCE AND FRICTION FACTOR OF VARIOUS NANOFLUIDS IN A DOUBLE-TUBE COUNTER FLOW HEAT EXCHANGER

by

Dan ZHEN[a], Jin WANG[a*], Yu PANG[a], Zhanxiu CHEN[b], and Bengt SUNDEN[c*]

[a]School of Energy and Environmental Engineering, Hebei University of Technology, Tianjin, China
[b]Key Laboratory of Efficient Utilization of Low and Medium Grade Energy (Tianjin University), Ministry of Education of China, Tianjin, China
[c]Department of Energy Sciences, Division of Heat Transfer, Lund University, Lund, Sweden

Original scientific paper
https://doi.org/10.2298/TSCI200323280Z

Experimental research was conducted to reveal the effects of nanofluids on heat transfer performance in a double-tube heat exchanger. With nanoparticle weight fraction of 0.5-2.0% and Reynolds number of 4500-14500, the flow resistance and heat transfer were analyzed by using six nanofluids, i.e., CuO-water, Al_2O_3-water, Fe_3O_4-water, ZnO-water, SiC-water, SiO_2-water nanofluids. Results show that SiC-water nanofluid with a weight concentration of 1.5% provides the best improvement of heat transfer performance. 1.0% CuO-water and 0.5% SiO_2-water nanofluids have lower friction factors in the range of Reynolds number from 4500-14500 compared to the other nanofluids. Based on test results of heat transfer performance and flow resistance, the 1.0% CuO-water nanofluid shows a great advantage due to a relatively high heat transfer performance and a low friction factor. Finally, empirical formulae of Nusselt numbers for various nanofluids were established based on experimental data tested in the double-tube heat exchanger.

Keywords*: nanofluids, double-tube heat exchanger, Nusselt number, flow resistance, empirical formulae*

Introduction

Considering that traditional heat transfer media cannot meet the demand of science and technology development, researchers have conducted extensive research on nanofluids. The concept of nanofluid was first mentioned by Choi [1]. Nanofluid is a new heat transfer medium with excellent thermal properties. Moreover, due to the nanoscale particle, it can reduce wears on the equipment. It has promising application prospects in many industrial fields. Gupta *et al*. [2] summarized the thermophysical properties of hybrid nanofluids, and Ranjbarzadeh *et al*. [3] investigated the stability of various nanofluids. Jilte *et al*. [4] conducted a comparison of nanofluid cooling performance by changing arrangements of cooling components. Results confirmed the applicability of these battery cooling systems in electric vehicles. Nazari *et al*. [5] experimentally investigated the effectiveness of Cu_2O nanofluid in a solar evaporator. They found that daily productivity of distilled water was

* Corresponding authors, e-mail: wjwcn00@163.com, bengt.sunden@energy.lth.se

enhanced by 23.7% using 0.04 vol.% Cu_2O nanofluid at 180 Lpm. Athinarayanan *et al*. [6] numerically investigated heat transfer enhancement in a confined adiabatic channel by using Cu-water nanofluid. It was found that the size of the symmetry vortices linearly increase with an increase of Reynolds number and nanoparticle volume fraction. Chen *et al*. [7] investigated the heat transfer characteristics of an electric heaters by using various nanofluids. Belahmadi and Bessaih [8] numerically investigated the entropy generation of Al_2O_3-water nanofluids in a coaxial cylinder under magnetic fields. They found that the magnetic field strength and direction played a decisive role on the entropy generation of the Al_2O_3-water nanofluids compared to other dimensionless parameters, such as Hartmann and Rayleigh numbers.

In addition, Duangthongsuk and Wongwises [9] found that the pressure drop increased with an increase of nanoparticles volume fraction. Abbasian Arani and Amani [10] conducted experiments to study the thermal performance and flow resistance of a counter-flow heat exchanger filled with TiO_2 nanofluids. Results revealed that with the nanofluid concentration increasing, the Nusselt number and pressure drop of nanofluids increased significantly. Zhang *et al*. [11] investigated rheological characteristics of nanofluids in a sudden expansion pipe. It was found that the loss coefficient, *K*, was kept constant with an increase of volume concentration. Hussein [12] investigated heat transfer characteristics of a double pipe heat exchanger filled with a hybrid nanofluid (mixture of aluminum nitride nanoparticles and ethylene glycol). It was concluded that the hybrid nanofluid drastically increased heat transfer performance of the heat exchanger, and a 35% increment was found at high volume fraction compared to the base fluid.

It is easily found that nanofluids have been widely studied in the open literature. Generally, few carbon-based compounds were used to prepare nanofluids in a single piece of research work, and related comparisons of heat transfer characteristics were rarely conducted in previous studies. In addition, most studies only showed the recommendation about the optimal nanofluid in a small optional scope. Due to different research backgrounds and experimental conditions, a comprehensive comparison of various nanofluids has not been accurately obtained in previous studies. This paper investigated thermal performance and flow resistance of six different nanofluids in a double-tube heat exchanger. Nusselt numbers and friction factors were analyzed with different Reynolds number and nanoparticle mass concentration.

Experimental method

Apparatus

As shown in fig. 1, the experimental system is mainly composed of a test section, a pressure gauge, a data logger, two water pumps, two thermostatic water baths, two water tanks and two flowmeters. A double-tube heat exchanger with a length of 1 m was used for the test section. The nanofluid and hot water flow in the inner tube and the annular outer part. The outer and inner tubes are made of stainless steel and copper. The inner tube has an inner diameter of 6 mm, and the thickness of the inner tube is 2 mm. The outer diameter of the outer tube is 16 mm. The test section is covered by insulating cotton to reduce heat loss. Thermocouples were used to measure temperature values at the inlet and exit. The pressure drop between the inlet and exit of the nanofluid was measured by using an U-tube. Inlet temperatures of the nanofluid and water were kept constant by using two water baths. The flow rates of the nanofluid and water were measured by flowmeters Titan 800 series, and flow control valves were used to adjust the flow rate.

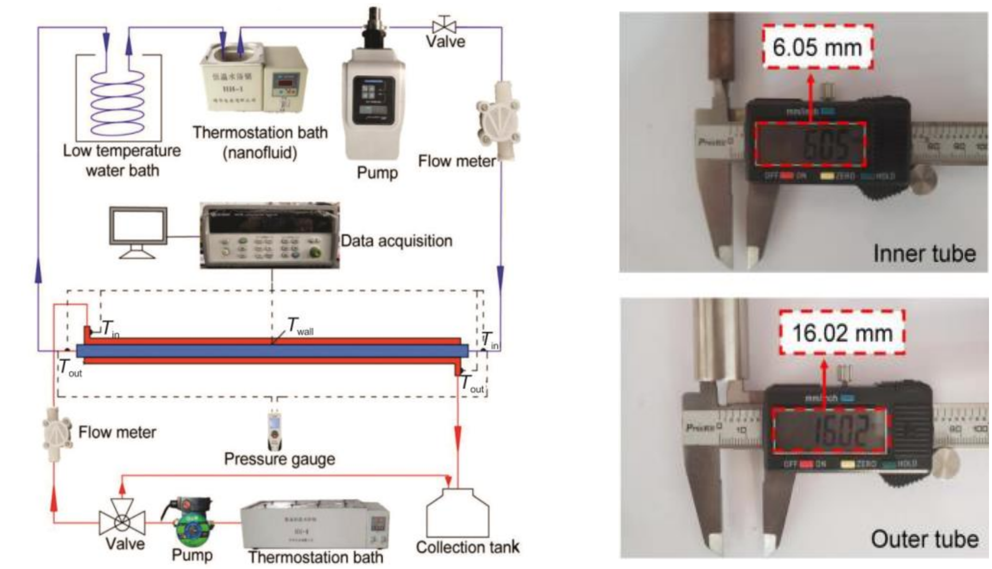

(a) **(b)**

Figure 1. Experimental system and dimensions of the tubes; (a) experimental system and (b) inner diameters of the test section

Sample preparation

In this work, a two-step method was adopted to prepare the nanofluids. All the nanoparticles (20 nm Al_2O_3, 40 nm CuO, 20 nm Fe_3O_4, 30 nm ZnO, 40 nm SiC, and 30 nm SiO_2) were purchased from the *Deke Daojin Company of China*, and they provided the information of thermodynamic properties and particle size.

Table 1. Thermodynamic properties of DI-water and nanoparticles

Materials	ρ [kgm^{-3}]	c_p [Jkg^{-1}K^{-1}]	$(\rho c_p)_{\text{particle}}(\rho c_p)_{\text{water}}$
DI-water	997	4180	1
Al_2O_3	3900	880	0.82
CuO	6500	540	0.84
Fe_3O_4	5180	670	0.83
ZnO	2901	923	0.64
SiC	3370	1340	1.08
SiO_2	2200	703	0.37

Table 1 shows the thermodynamic properties of the nanoparticles and deionized water (DI-water). The mass concentrations of the prepared nanofluids are 0.5 wt.%, 1.0 wt.%, 1.5 wt.%, and 2.0 wt.%. Nanoparticles are first added into DI-water and mechanically stirred for 10 minute. Sodium hexametaphosphate (SHMP) and hexadecyl trimethyl ammonium bromide (CTMAB) were used as dispersant to improve stability of nanofluids. Finally, the ultrasonic vibration is used for the mixed fluid to avoid agglomeration of particles. After 10 days standing, absolute values of Zeta (δ) potentials are 39.8 mV, 34.5 mV, 31.9 mV, 33.7 mV, 31.9 mV, and 31.7 mV for the water-based Al_2O_3, CuO, Fe_3O_4, ZnO, SiC, and SiO_2 nanofluids with a mass fraction of 2.0 wt.%, respectively. This result indicates that the used nanofluids in the study show good stability. Figure 2 shows photographs of nanoparticles and nanofluids by using transmission electron microscopy (TEM).

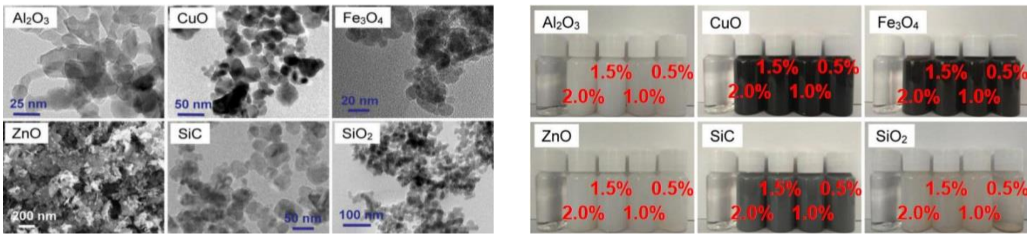

(a) (b)

Figure 2. The TEM photos of nanoparticles and pictures of nanofluids; (a) six nanoparticles, (b) samples of six nanofluids

Data analysis

In order to investigate Nusselt number and flow resistance of various nanofluids, the heat transfer rate from the hot fluid (water) is calculated by:

$$Q_\mathrm{w} = m_\mathrm{w} c_{p,\mathrm{w}} \left(T_\mathrm{in} - T_\mathrm{out}\right)_\mathrm{w} \tag{1}$$

where Q_w and m_w represent the heat transfer rate and the mass-flow rate of the hot water, respectively. Symbols $c_{p,\mathrm{w}}$, T_out, and T_in each represent the specific heat of hot water, the temperatures of hot water at the inlet and outlet. The heat transfer rate from the nanofluid is defined:

$$Q_\mathrm{nf} = m_\mathrm{nf} c_{p,\mathrm{nf}} \left(T_\mathrm{out} - T_\mathrm{in}\right)_\mathrm{nf} \tag{2}$$

where Q_nf, m_nf, and $C_{p,\mathrm{nf}}$ each represent the heat transfer rate, the mass-flow rate, and the specific heat of the nanofluid. The T_out and T_in are temperature values of the nanofluid at the inlet and the outlet, respectively. The Q_ave represents the average heat transfer rate of the heat transfer media (water and nanofluid), which is calculated:

$$Q_\mathrm{ave} = \frac{Q_\mathrm{w} + Q_\mathrm{nf}}{2} \tag{3}$$

The nanofluid bulk temperature T_nf is calculated by eq. (4). Reynolds number, heat transfer coefficient, and Nusselt number for the nanofluid are calculated:

$$T_\mathrm{nf} = \frac{\left(T_\mathrm{out} + T_\mathrm{in}\right)_\mathrm{nf}}{2} \tag{4}$$

$$\mathrm{Re}_\mathrm{nf} = \frac{\rho_\mathrm{nf} u D}{\mu_\mathrm{nf}} \tag{5}$$

$$h_\mathrm{nf} = \frac{Q_\mathrm{ave}}{A_i \left(T_\mathrm{wall} - T_\mathrm{nf}\right)} \tag{6}$$

$$\mathrm{Nu}_\mathrm{nf} = \frac{h_\mathrm{nf} D}{k_\mathrm{nf}} \tag{7}$$

where ρ_nf is the nanofluid density, u – the nanofluid mean velocity, D – the inner diameter of the testing tube. The μ_nf, h_nf, and A_i each represent the nanofluid viscosity, the heat transfer coefficient of the nanofluid, and the inner tube area, T_wall – the wall temperature, Nu_nf and k_nf are the Nusselt number and the thermal conductivity of the nanofluid, respectively.

When the nanofluid flows through the test section, the nanofluid friction factor is calculated by:

$$f_{\mathrm{nf}} = \frac{2D\Delta P_{\mathrm{nf}}}{L\rho_{\mathrm{nf}}u^2} \tag{8}$$

where f_{nf}, ΔP_{nf} and L each represent the friction factor, the measured pressure drop and the length of the test tube. The physical properties of the nanofluid are calculated as in [13, 14] and read:

$$\rho_{\mathrm{nf}} = (1-\phi)\rho_f + \phi\rho_p \tag{9}$$

$$\left(\rho c_p\right)_{\mathrm{nf}} = (1-\phi)\left(\rho c_p\right)_{\mathrm{f}} + \phi\left(\rho c_p\right)_{\mathrm{p}} \tag{10}$$

$$\mu_{\mathrm{nf}} = \mu_{\mathrm{f}}\,(1+2.5\phi) \tag{11}$$

$$\frac{k_{\mathrm{nf}}}{k_{\mathrm{f}}} = \frac{k_p + 2k_{\mathrm{f}} + 2\phi\left(k_{\mathrm{f}} - k_{\mathrm{p}}\right)}{k_p + 2k_{\mathrm{f}} - \phi\left(k_{\mathrm{f}} - k_{\mathrm{p}}\right)} \tag{12}$$

where ρ_{p} and ρ_{f} are the density of nanoparticles and DI-water, respectively, μ_{f} – the viscosity of DI-water, k_{p}, k_{f}, and ϕ are thermal conductivities of nanoparticles, DI-water, and the volume fraction of the nanofluid, respectively.

Uncertainty analysis

In the present study, uncertainty of the experimental results is determined by the deviations of the measured parameters. The calculation of the uncertainty is based on the study of error propagation described by Moffat [15]. Uncertainties of the experimental measurements are listed in tab. 2.

Table 2. Uncertainty analysis for results

Variable name	Uncertainty
Length, *L*	±0.0001 m
The inner of the inner tube, *D*	±0.0001 m
Mass of nanoparticles	±0.001 g
Thermocouple measuring temperature	±0.1 ºC
Volume flow	±2%
Pressure drop	±0.3%
Heat transfer rate	±2.04%
Convective heat transfer coefficient	±2.66%
Reynolds number	±2.6%
Friction factor, *f*	±2.62%
Nusselt number	±3.15%

The uncertainties of heat transfer rate, convective heat transfer coefficient, Reynolds number, friction factor and Nusselt number are determined by:

$$U_Q = \left[\left(\frac{\Delta\dot{m}}{\dot{m}}\right)^2 + \left(\frac{\Delta c_p}{c_p}\right)^2 + \left(\frac{\Delta T}{T}\right)^2\right]^{1/2} \tag{13}$$

$$U_h = \left[\left(\frac{\Delta Q}{Q}\right)^2 + \left(\frac{\Delta A}{A}\right)^2 + \left(\frac{\Delta T}{T}\right)^2\right]^{1/2} \tag{14}$$

$$U_{\mathrm{Re}} = \left[\left(\frac{\Delta\rho}{\rho}\right)^2 + \left(\frac{\Delta u}{u}\right)^2 + \left(\frac{\Delta\mu}{\mu}\right)^2 + \left(\frac{\Delta D}{D}\right)^2\right]^{1/2} \tag{15}$$

$$U_f = \left[\left(\frac{\Delta P}{P}\right)^2 + \left(\frac{\Delta\rho}{\rho}\right)^2 + \left(\frac{\Delta u}{u}\right)^2 + \left(\frac{\Delta\mu}{\mu}\right)^2 + \left(\frac{\Delta D}{D}\right)^2 + \left(\frac{\Delta L}{L}\right)^2\right]^{1/2} \tag{16}$$

$$U_{Nu} = \left[\left(\frac{\Delta h}{h}\right)^2 + \left(\frac{\Delta k}{k}\right)^2 + \left(\frac{\Delta D}{D}\right)^2\right]^{1/2} \tag{17}$$

Verification of experimental results

Nusselt number and friction factor of DI-water were compared to those obtained by existing empirical formulae in Naphon *et al*. [16]. These empirical formulas are given:

$$\mathrm{Nu} = 1.84(\mathrm{Re} - 1500)^{0.32}\,\mathrm{Pr}^{0.07} \tag{18}$$

$$f = 0.66\mathrm{Re}^{-0.33} \tag{19}$$

Figure 3 shows experimental data and empirical values of the friction factors and the Nusselt numbers. It is found that the errors of the Nusselt number between the experimental data and the empirical values is below 4%, and difference of friction factors between experimental data and empirical value is less than 5%. This finding shows that the experimental values of the DI-water have good agreement with the empirical ones.

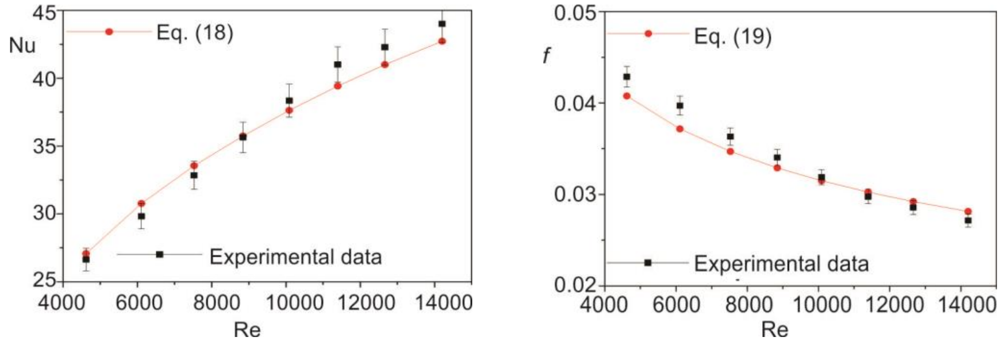

(a) (b)

Figure 3. Comparisons of Nusselt numbers and friction factors between experimental tests and calculated values in eqs. (18) and (19); (a) Nusselt number, (b) friction factors

Results and discussion

The experimental conditions are given as follows: for the six nanofluids, the Reynolds number ranges from approximately 4000-14500, and the nanofluid inlet temperature is 25 °C. The water inlet temperature is 60 °C, and the water mass-flow rate is 2 Lpm. In this research, the maximum relative difference between Q_w and Q_{nf} is 5.17% for the 2.0 wt.% ZnO nanofluid with a mass-flow of 2 Lpm.

Analysis of Nusselt number

A comparison of Nusselt numbers between DI-water and various nanofluids is conducted by considering an effect of mass fraction as shown in fig. 4. It indicates that with the increase of the Reynolds number from 4500-14500, the Nusselt number increases significantly for all the tested nanofluids.

Figure 4(a) presents the Nusselt numbers of the Al_2O_3-water nanofluid with various mass fractions at different Reynolds numbers. From the results, the Nusselt number increases with an increase of nanoparticle mass fraction as other nanofluids. While the Nusselt number growth is inconspicuous in the scope of the test range relative to DI-water. For Al_2O_3-water nanofluid with test mass fractions, the Nusselt number is lower than that of DI-water at Re = 4500. The 1.5% Al_2O_3-water nanofluid shows a similar heat transfer performance as DI-water at a lower Reynolds number (below 12000). The nanofluid with 2.0% mass fraction shows the best thermal performance, and in this case a 12.2% increment of Nusselt number is obtained compared to the DI-water at Re = 14500. Considering the high cost of nanoparticles, the Al_2O_3-water nanofluid with a high mass fraction is not recommended for improvement of thermal performance of double-tube heat exchangers.

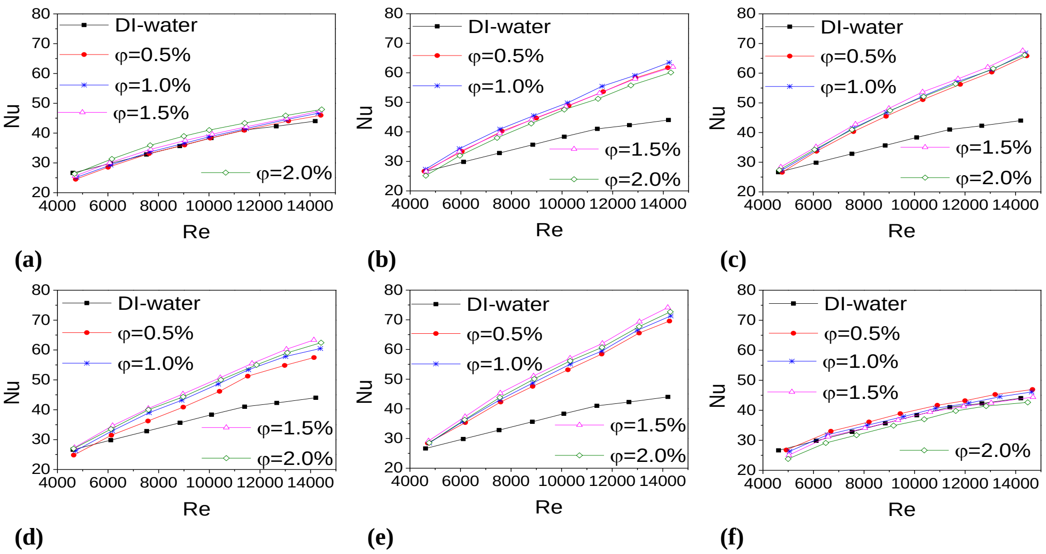

Figure 4. Nusselt numbers for DI-water and various nanofluids; (a) Al_2O_3-water nanofluid, (b) CuO-water nanofluid, (c) Fe_3O_4-water nanofluid, (d) ZnO-water nanofluid, (e) SiC-water nanofluid, (f) SiO2-water nanofluid
(-■-: DI-water, -●-: *φ* = 0.5%, -*-: *φ* = 0.5% -△-: *φ* = 1.5%, -◇-: *φ* = 2.0%)

Figure 4(b) shows that variations of Nusselt number for CuO-water nanofluid under effects of Reynolds numbers and particle concentration. As the concentration of the CuO particles increases, the Nusselt number of CuO-water nanofluid increases first and then decreases, and 1.0% mass concentration of CuO-water nanofluids shows the highest Nusselt number compared with DI-water and CuO-water nanofluids with other mass concentrations. Compared with DI-water at Re = 4500-14500, the Nusselt number of CuO-water nanofluids with 1.0% mass concentration is increased by 2.63% and 44.3%, respectively. The results indicate that adding nanoparticles to DI-water not only plays an active role in thermal conductivity of mixed fluid but also results in a significant increment in viscosity, which was significant effects on thermal performance of the double-tube heat exchanger.

Figures 4(c)-4(e) analyze variations of Nusselt numbers for various Fe_3O_4-water, ZnO-water and SiC-water nanofluids at various flow conditions. With a test range of 0.5-2.0 wt.%, the Nusselt number of these nanofluids increases with the increase of the flow rate, and the maximum value of the Nusselt number is observed for the cases with 1.5% mass concentration. The effect of the mass concentration on the heat transfer performance of the Fe_3O_4-water nanofluid is negligible. Compared with the DI-water at the Reynolds numbers of 4500 and 14500, the Nusselt numbers of the 1.5% Fe_3O_4-water nanofluids increase by 6.5% and 53.5%. The increases of the Nusselt numbers for the 1.5% ZnO-water nanofluids are

2.55% and 43.0% compared to DI-water at the Reynolds numbers 4500 and 14500. At the Reynolds number of 4500, the DI-water shows higher values of Nusselt number than 0.5 wt.% ZnO-water nanofluid. The Nusselt numbers of the 1.5% SiC-water nanofluids at the Reynolds numbers 4500 and 14200 are 9.64% and 68.4% higher than those of the DI-water. For these three nanofluids with 1.5% mass fraction, the SiC-water nanofluid shows the optimal heat transfer performance, whereas the ZnO-water nanofluid shows the worst heat transfer performance (due to smaller values of Nu compared to others).

For SiO_2-water nanofluid, variations of Nusselt numbers with Reynolds number are shown in fig. 4(f). Results indicate that the Nusselt number decreases with the increase of the mass concentration for SiO_2-water nanofluid. The maximum enhancement of the Nusselt number of SiO_2-water nanofluids is observed at 0.5% mass fraction, and the improvement is about 6.6% at Re = 14500. Especially for the 2.0 wt.% SiO_2-water nanofluid, the Nusselt number shows lower values than for the DI-water.

This result indicates that there might be more agglomeration and sedimentation of particles when the DI-water is mixed with 2.0 wt.% SiO_2 nanoparticles. Compared with other particles, adding Al_2O_3 and SiO_2 nanoparticles into DI-water reveals slight influence on thermal enhancement. In other words, it is found that adding nanoparticles with high thermal conductivity into the base fluid will improve thermal performance of base fluid. Moreover, irregular movements of nanoparticles will destroy the thermal boundary layer, which enhances the heat transfer between hot water and nanofluid.

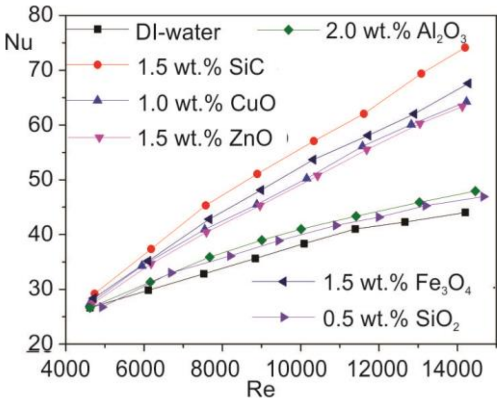

Figure 5. Comparisons of Nusselt numbers for various nanofluids at Re = 4500-14500.

It is found that the 2.0% Al_2O_3-water, 1.0% CuO-water, 1.5% Fe_3O_4-water, 1.5% ZnO-water, 1.5% SiC-water, 0.5% SiO_2-water nanofluids obtain the highest Nusselt numbers, compared with other nanoparticle concentrations in the range 0.5~2.0%. These results indicate that particle agglomeration appears when the nanoparticle mass concentration exceeds a certain value. To confirm the nanofluid with the best thermal performance, a comparison of six nanofluids with the optimal mass concentration is further conducted in fig. 5 These results show that the 1.5% SiC-water nanofluid shows the most increment in heat transfer.

Analysis of friction factor

Figure 6 shows that the friction factors of various nanofluids decrease by increasing Reynolds number and decreasing the nanoparticle mass fraction. It is easily observed that the six nanofluids have higher friction factors than the DI-water. Figure 6(a) presents the friction factors of the Al_2O_3-water nanofluid with different mass fractions. The 2.0% Al_2O_3-water nanofluid has the largest flow resistance, and these friction factors at the Reynolds numbers 4500 and 14500 increase by 53.4% and 34.9% compared to the DI-water. As shown in fig. 6(b), compared with the DI-water at Reynolds numbers 4500 and 14500, the friction factors of the 2.0% CuO-water nanofluid increase by 45.5% and 32.1%. Figure 6(c) presents values of the friction factors for the Fe_3O_4-water nanofluids. The 2.0% Fe_3O_4-water nanofluid has the largest flow resistance. Compared with the DI-water, corresponding increases of 73.1%

and 42.5% are obtained at the Reynolds numbers 4500 and 14500. Performance of the flow resistance for the ZnO-water nanofluid is presented in fig. 6(d). At the Reynolds numbers 4500 and 14500, the friction factors of the 2.0% ZnO-water nanofluid are 73.5% and 52.6% higher than these of the DI-water. Compared with the DI-water, the friction factors of the SiC-water nanofluids with 2.0% mass concentration increase by 77.6% and 49.8% at the Reynolds numbers 4500 and 14400. Figure 6(f) shows the friction factors for the SiO_2-water nanofluids with various mass concentrations, and influence of mass concentration on the flow resistance is inconspicuous. Increases of friction factors for the 2.0% SiO_2-water nanofluids are about 46.4% and 31.9% at the Reynolds numbers 4500 and 14500.

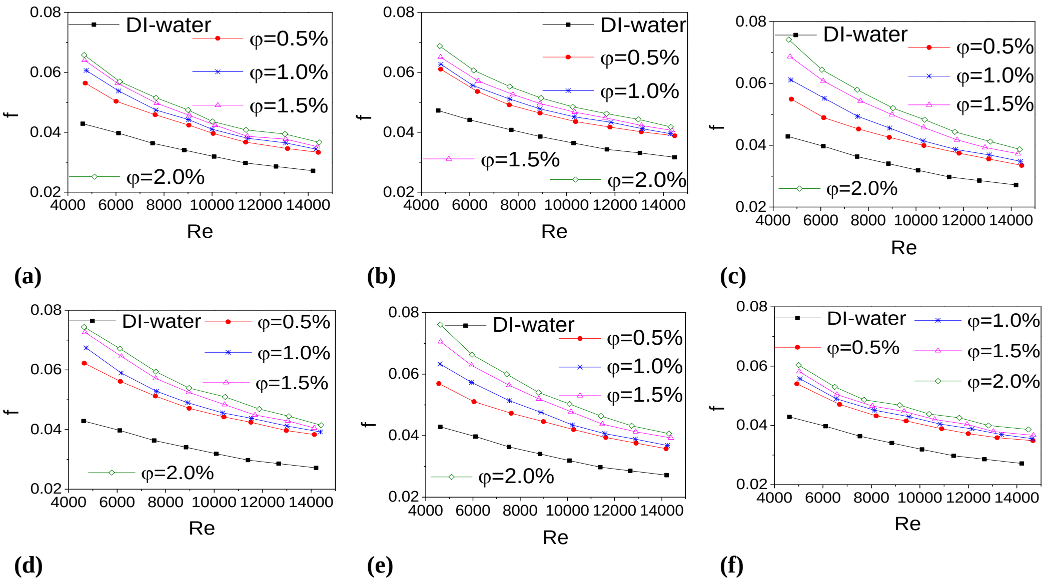

Figure 6. Friction factors for both DI-water and various nanofluids; (a) Al_2O_3-water nanofluid, (b) CuO-water nanofluid, (c) Fe_3O_4-water nanofluid, (d) ZnO-water nanofluid, (e) SiC-water nanofluid, (f) SiO_2-water nanofluid
(-■-: DI-water, -●-: φ = 0.5%, -*-: φ = 0.5% -△ -: φ = 1.5%, -◇ -: φ = 2.0%)

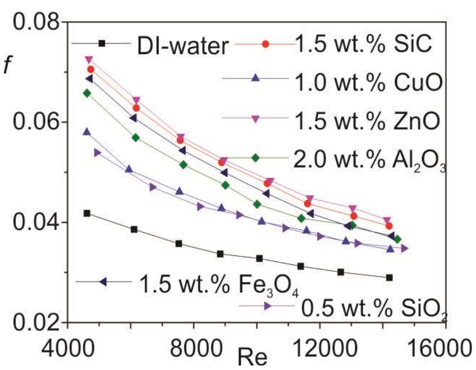

Figure 7. Comparison of friction factors for various nanofluids at Re = 4500-14500

These results are because adding nanoparticles leads to an increase in the fluid viscosity, which decreases flow diffusion. Results indicate that the nanoparticle mass fraction shows more significant influence on Fe_3O_4, ZnO, and SiC water-based nanofluids than other three cases. Figure 7 shows further comparisons of thermal performance and flow resistance of the six nanofluids. These results indicate that the 1.0% CuO-water and 0.5% SiO_2-water nanofluids have lower friction factors at Re = 4500-14500. For the six nanofluids with the optimum concentration, detailed results about thermal performance and flow resistance are shown in tab. 3.

Table 3. Increments of Nusselt number and friction factor for the six nanofluids

Nanofluid	Mass fraction	Enhancement of Nusselt number	Increase of friction factor
Al_2O_3-water	2.0 wt.%	–8%~12.2%	34.9%~53.5%
CuO-water	1.0 wt.%	2.6%~44.3%	24.9%~32.7%
Fe_3O_4-water	1.5 wt.%	6.5%~53.5%	37.3%~60.3%
ZnO-water	1.5 wt.%	2.2%~43.0%	49.2%~69.4%
SiC-water	1.5 wt.%	9.6%~68.4%	44.6%~64.6%
SiO_2-water	0.5 wt.%	0.5%~32.7%	26.0%~28.3%

The reason is that increments in both thermal conductivity and viscosity of the nanofluid are obtained by increasing the particle mass fraction. An increase in thermal conductivity will lead to a positive effect on thermal performance of the nanofluid, and an increase in fluid viscosity will deteriorate an enhancement in heat transfer. When nanoparticle concentration is less than the optimum concentration value, the effect of the high thermal conductivity and less nanoparticle agglomeration is larger than the viscosity inhibition effect. When the nanoparticle concentration is larger than the optimum value, the viscosity inhibition effect is stronger than that increase in the thermal conductivity, which decreases the nanofluid heat transfer performance.

In addition, for nanofluids at a low Reynolds number, the increment in viscosity is larger than that in thermal conductivity, and Nusselt number shows lower values compared to the DI-water. With increases of Reynolds number and mass concentration, the enhancement of thermal conductivity shows higher influence than the viscosity inhibition. Based on discussions about figs. 5 and 7 and tab. 3, the 1.0% CuO-water nanofluid shows a relatively high heat transfer rate (only less than SiC and Fe_3O_4 water-based nanofluids) with a low friction factor of 24.9~32.7% in Re = 10000-14500. Therefore, the 1.0% CuO-water nanofluid is recommended as a working medium inside a double-tube exchanger due to a relatively a better thermal performance and a lower friction factor.

Empirical formula

In this part, empirical formulae of Nusselt numbers for six nanofluids in the double-tube heat exchanger are summarized by considering effects of different mass concentrations. Generally, it is recommended that the Nusselt number of nanofluids can be predicted by:

$$\mathrm{Nu} = a\,\mathrm{Re}^{\mathrm{b}}\,\mathrm{Pr}^{\mathrm{c}} \tag{20}$$

In the present study, a new finding is that there is the best mass fraction for the Nusselt number increments. Nusselt number is increased by increasing mass fraction, when concentration is below the optimum value. However, the trend will be reversed when the mass concentration is above this value). The effect of the optimum values for various nanofluids is also considered in the empirical formula as:

$$\mathrm{Nu} = a\,\mathrm{Re}^{\mathrm{b}}\,\mathrm{Pr}^{\mathrm{c}}\left[1+\left(\left|\phi-d\right|\right)^{\mathrm{e}}\right] \tag{21}$$

where φ and d represent the mass concentration and the optimum mass concentration value for every nanofluid, respectively. The ranges of the equivalent Reynolds number, Prandtl number and mass fraction are $4500 \leq \mathrm{Re} \leq 14500$, $5 \leq 4\mathrm{Pr} \leq 8$, and $0.5\% \leq 8\varphi \leq 82.0\%$. Table 4 shows the values of the variables a, b, c, d, and e for the different nanofluids.

Table 4. Variables of empirical formulae for six nanofluids

Nanofluid	a	b	c	d	e
Al_2O_3-water	0.1	0.5	0.76	0	0.55
CuO-water	0.022	0.67	0.91	0.01	0.7
Fe_3O_4-water	0.04	0.68	0.54	0.015	0.8
ZnO-water	0.03	0.59	1.22	0.015	0.37
SiC-water	0.013	0.75	0.86	0.015	0.66
SiO_2-water	0.19	0.15	0.55	0.005	0.66

Conclusions

In this paper, effects of Reynolds number and mass concentration on the thermal performance and flow characteristics of nanofluids were investigated in a double-tube heat exchanger. According to the experimental results, several conclusions are summarised as follows:

- There is a peak of optimal nanoparticle mass concentration. It is found that for the concentration range of 0.5%-2.0%, the 2.0% Al_2O_3-water, 1.0% CuO-water, 1.5% Fe_3O_4-water, 1.5% ZnO-water, 1.5% SiC-water, 0.5% SiO_2-water nanofluids show the highest Nusselt numbers.
- It is found that the nanoparticle mass concentration was a great influence on ZnO-water, SiC-water nanofluids and Fe_3O_4-water nanofluids. The 1.0% CuO and the 0.5% SiO_2 water-based nanofluids have similar friction factors especially in the Re = 10000-14500, and friction factors of these two fluids are lower than the other ones.
- Based on comparisons of six nanofluids, at the Reynolds numbers 4500 and 14500, 1.0% CuO-water nanofluid shows a relatively high heat transfer rate (2.6%~44.3% increments of Nusselt number) and a low friction factor (24.9%~32.7% increments of friction factor).

Finally, this research presents empirical formulae which can predict the Nusselt number of six nanofluids under certain conditions. These provide ways to investigate the thermal performance of various nanofluids filled in a double-tube heat exchanger.

Acknowledgment

This work is supported by Open Foundation Program of Key Laboratory of Efficient Utilization of Low and Medium Grade Energy (Tianjin University), Ministry of Education of China [Grant No. 201503-404] and the Natural Science Foundation of Hebei Province of China [Grant No. E2019202184].

Nomenclature

c_p – specific heat [$\mathrm{Jkg^{-1}K^{-1}}$]
D – tube diameter [mm]
f – friction factor
h – convective heat transfer coefficient [$\mathrm{Wm^{-2}K^{-1}}$]
k – thermal conductivity [$\mathrm{Wm^{-1}K^{-1}}$]
L – length of the test tube [m]
$\dot{m}$ – mass-flow rate [$\mathrm{kgs^{-1}}$]
Nu – Nusselt number [= hDk^{-1}][−]
ΔP – pressure drop [Pa]
Pr – Prandtl number [= $\mu c_p k^{-1}$][−]
q – heat flux [$\mathrm{Wm^{-2}}$]
Q – heat transfer rate [W]
Re – Reynolds number [= $\rho u D \mu^{-1}$][−]
T – temperature [ºC]
u – mean velocity [$\mathrm{ms^{-1}}$]

Greek symbols

μ – viscosity [$\mathrm{kgm^{-1}s^{-1}}$]
ρ – density [$\mathrm{kgm^{-3}}$]
ϕ – nanoparticle volume concentration

Subscripts

ave – average
f – base fluid
in – inlet
nf – nanofluid
out – outlet

Reference

[1] Choi, U. S., Enhancing Thermal Conductivity of Fluid with Nanoparticles, in: *Development and Application of Non-Newtonian Flows*, (Eds. D. A. Singiner, H. P. Wang), FED– Vol. 231/MD– Vol. 66, The American Society of Mechanical Engineers, New York, USA, 1995, pp. 99-105

[2] Gupta, M., *et al.*, Up to Date Review on the Synthesis and Thermophysical Properties of Hybrid Nanofluids, *J. Clean. Prod.*, *190* (2018), July, pp. 169-192

[3] Ranjbarzadeh, R., *et al.*, An Experimental Study on Stability and Thermal Conductivity of Water/Silica Nanofluid: Eco-Friendly Production of Nanoparticles, *J. Clean. Prod.*, *206* (2019), Jan., pp. 1089-1100

[4] Jilte, R. D., *et al.*, Cooling Performance of Nanofluid Submerged vs. Nanofluid Circulated Battery Thermal Management Systems, *J. Clean. Prod.*, 240 (2019), Dec., 118131

[5] Nazari, S., *et al.*, Performance Improvement of a Single Slope Solar Still by Employing Thermoelectric Cooling Channel and Copper Oxide Nanofluid: An Experimental Study, *J. Clean. Prod.*, *208* (2019), Jan., pp. 1041-1052

[6] Athinarayanan, A. S. K., *et al*., Numerical Investigation of Heat Transfer from Flow over Square Cylinder Placed in a Confined Channel Using Cu−Water Nanofluid, *Thermal Science*, *23* (2019) Suppl. 4, pp. S1367-S1380

[7] Chen, Z. X., *et al*., Experimental Investigation on Heat Transfer Characteristics of Various Nanofluids in an Indoor Electric Heater, *Renew. Energy*, *147* (2020), Part I, pp. 1011-1018

[8] Belahmadi, E., Bessaih, R., Entropy Generation Analysis of Nanofluid Natural Convection in Coaxial Cylinders Subjected to Magnetic Field, *Thermal Science*, *23* (2018), 6A, pp. 3467-3479

[9] Duangthongsuk, W., Wongwises, S., An Experimental Study on the Heat Transfer Performance and Pressure Drop of TiO_2-Water Nanofluids Flowing under a Turbulent Flow Regime, *Int. J. Heat Mass Transf.*, *53* (2010), 1-3, pp. 334-344

[10] Abbasian Arani, A. A., Amani, J., Experimental Study on the Effect of TiO_2–Water Nanofluid on Heat Transfer and Pressure Drop, *Exp. Therm. Fluid Sci.*, *42* (2012), Oct., pp. 107-115

[11] Zhang, H. C., *et al*., Flow and Heat Transfer Characteristics of Nanofluids in Sudden Expansion Structure Based on SLA Method, *Thermal Science*, *23* (2019), 3A, pp. 1449-1455

[12] Hussein, A. M., Thermal Performance and Thermal Properties of Hybrid Nanofluid Laminar Flow in a Double Pipe Heat Exchanger, *Exp. Therm. Fluid Sci.*, *88* (2017), Nov., pp. 37-45

[13] Pak, B. C., Cho, Y. I., Hydrodynamic and Heat Transfer Study of Dispersed Fluids with Submicron Metallic Oxide Particles, *Exp. Therm. Fluid Sci.*, *11* (1998), 2, pp. 151-170

[14] Xuan, Y. M., Roetzel, W., Conceptions for Heat Transfer Correlation of Nanofluids, *Int. J. Heat Mass Transf.*, *43* (2000), 19, pp. 3701-3707

[15] Moffat, R. J., Describing the Uncertainties in Experimental Results, *Exp. Therm. Fluid Sci.*, *1* (1988), 1, pp. 3-17

[16] Naphon, P., *et al*., Tube Side Heat Transfer Coefficient and Friction Factor Characteristics of Horizontal Tubes with Helical Rib, *Energy Convers. Manag.*, *47* (2006), 18-19, pp. 3031-3044

Paper submitted: March 24, 2020
Paper revised: June 26, 2020
Paper accepted: August 1, 2020